AD-A058 305 LOCKHEED MISSILES AND SPACE CO INC PALO ALTO CALIF PA--ETC F/G 20/1
STAGGERED SOLUTION PROCEDURES FOR DOUBLY ASYMPTOTIC FLUID-STRUC--ETC(U)
FEB 78 K C PARK, C A FELIPPA, J A DERUNTZ DNA001-76-C-0285

UNCLASSIFIED LMSC/D624324 DNA-4525F NL

1 OF 1
AD
A058305

END
DATE
FILMED
10-78
DDC

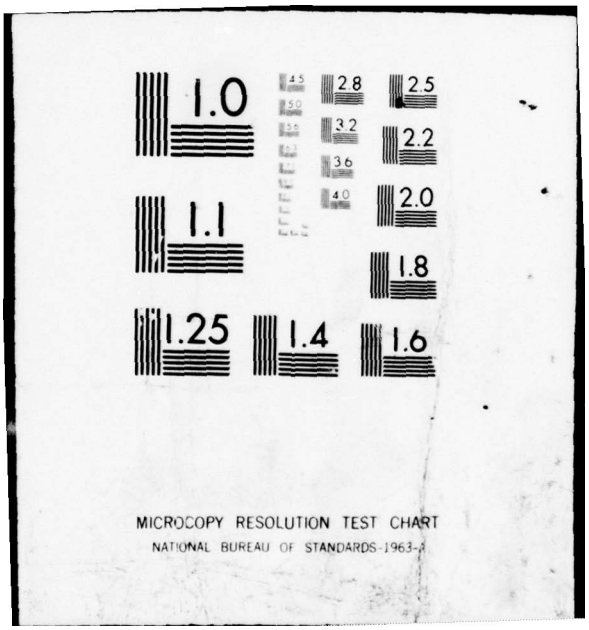
1.0
1.1
1.25
1.4
1.6
1.8
2.0
2.2
2.5
2.8
3.2
3.6
4.0
4.5
5.0
MICROCOPY RESOLUTION TEST CHART
NATIONAL BUREAU OF STANDARDS-1963-A

(12) LEVEL II

DNA 4525F

STAGGERED SOLUTION PROCEDURES FOR DOUBLY ASYMPTOTIC FLUID-STRUCTURE INTERACTION ANALYSIS

Lockheed Palo Alto Research Laboratory
3251 Hanover Street
Palo Alto, California 94304

28 February 1978

Final Report for Period 26 April 1976—28 February 1978

CONTRACT No. DNA 001-76-C-0285

THIS WORK SPONSORED BY THE DEFENSE NUCLEAR AGENCY
UNDER RDT&E RMSS CODE B344076462 L02BAXYX97801 H2590D.

Prepared for
Director
DEFENSE NUCLEAR AGENCY
Washington, D. C. 20305

Destroy this report when it is no longer
needed. Do not return to sender.

(18) DNA, SBIE

UNCLASSIFIED

SECURITY CLASSIFICATION OF THIS PAGE *(When Data Entered)*

(19) **REPORT DOCUMENTATION PAGE**

READ INSTRUCTIONS BEFORE COMPLETING FORM

1. REPORT NUMBER: DNA 4525F, AD-E300 309
2. GOVT ACCESSION NO.
3. RECIPIENT'S CATALOG NUMBER (9)

4. TITLE *(and Subtitle)* (6): STAGGERED SOLUTION PROCEDURES FOR DOUBLY ASYMPTOTIC FLUID-STRUCTURE INTERACTION ANALYSIS.

5. TYPE OF REPORT & PERIOD COVERED: Final Report for Period 26 Apr 76—28 Feb 78,

6. PERFORMING ORG. REPORT NUMBER: LMSC-D624324 (14)

7. AUTHOR(s) (10): K. C. Park, C. A. Felippa, J. A. DeRuntz

8. CONTRACT OR GRANT NUMBER(s) (15): DNA 001-76-C-0285

9. PERFORMING ORGANIZATION NAME AND ADDRESS: Lockheed Palo Alto Research Laboratory, 3251 Hanover Street, Palo Alto, California 94304 (17) X978

10. PROGRAM ELEMENT, PROJECT, TASK AREA & WORK UNIT NUMBERS (16): Subtask L02BAXYX978-01

11. CONTROLLING OFFICE NAME AND ADDRESS: Director, Defense Nuclear Agency, Washington, D.C. 20305

12. REPORT DATE (11): 28 February 1978

13. NUMBER OF PAGES: 52

14. MONITORING AGENCY NAME & ADDRESS *(if different from Controlling Office)* (12) 49p.

15. SECURITY CLASS *(of this report)*: UNCLASSIFIED

15a. DECLASSIFICATION/DOWNGRADING SCHEDULE

16. DISTRIBUTION STATEMENT *(of this Report)*

Approved for public release; distribution unlimited.

17. DISTRIBUTION STATEMENT *(of the abstract entered in Block 20, if different from Report)*

18. SUPPLEMENTARY NOTES

This work sponsored by the Defense Nuclear Agency under RDT&E RMSS Code B344076462 L02BAXYX97801 H2590D.

19. KEY WORDS *(Continue on reverse side if necessary and identify by block number)*

Fluid-Structure Interaction
Staggered Solution Procedures
Numerical Stabilization
Doubly Asymptotic Approximations

20. ABSTRACT *(Continue on reverse side if necessary and identify by block number)*

This report examines direct time integration techniques for the transient response analysis of fluid-structure interaction problems treated with the Doubly Asymptotic Approximation. Efficient solution of the equations of motion is achieved by a modular computer implementation in which separate fluid and structure analyzers are interfaced through extrapolation of the coupling terms. Because conventional realization of this technique is handicapped by severe time-increment limitations, a versatile formulation is developed that circumvents such limitations, achieving unconditional stability.

DD FORM 1 JAN 73 1473 EDITION OF 1 NOV 65 IS OBSOLETE

UNCLASSIFIED

SECURITY CLASSIFICATION OF THIS PAGE *(When Data Entered)*

PREFACE

The authors express their appreciation to Dr. T. L. Geers for his counseling during the performance of the work reported herein.

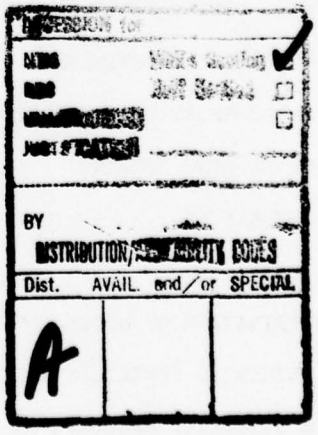

TABLE OF CONTENTS

LIST OF ILLUSTRATIONS

LIST OF TABLES

SECTION 1

INTRODUCTION

In recent years, increasing use has been made of the Doubly Asymptotic Approximation (DAA) [1-3] for the transient response analysis of submerged structures. Application of the DAA in conjunction with discrete methods of structural analysis leads to a large set of coupled ordinary differential equations (ODE) in time. Such equations are either solved directly in terms of the physical coordinates, or indirectly through a dimensionality-reduction transformation from physical to generalized coordinates. This report deals exclusively with the first approach.

The physical coordinates associated with the direct time integration approach are the response degrees-of-freedom of the structural model (the structural displacements) and the nodal values of the scattered pressure field at the contact surface (the fluid pressures). Fluid-structure interaction effects result in the coupling of the fluid pressures and structural displacements normal to the contact surface (the "wet displacements") through a matrix differential equation.

1.1 SOLUTION PROCEDURES

Three general schemes can be followed for organizing the response calculations:

- Pressure Elimination Solution. Elimination of the fluid pressure equations results in a differential system of equations in the structural displacements only; this system is of third order in time.
- Simultaneous Solution. The fully coupled system is processed as one entity, i.e., both displacements and pressures are simultaneously advanced through the use of a fully-implicit integration scheme.
- Staggered Solution. The integration process is carried out in alternating stages: the solution of either the structural or fluid system is advanced first, then the other system is solved following a time extrapolation of the coupling term(s) as a forcing function.

The first approach has the advantage of reducing the number of equations to be solved, but introduces unsymmetric coefficient matrices that are fully populated in entry positions pertaining to the "wet" degrees of freedom. Furthermore, the appearance of third-order (or higher) temporal derivatives of the displacement coordinates causes numerical difficulties in the treatment of initial and jump conditions in shock-excited problems. (These difficulties can be eliminated by passing to integro-differential forms, but then time integrals of applied forcing terms must be carried along in the calculations.)

The second approach can be organized in terms of symmetric matrices and does not require special treatment to account for acceleration-derivative terms. Processing times

for large-scale problems become rapidly prohibitive, even in linear analysis, on account of the matrix connectivity introduced by pressure/wet-displacement coupling blocks that may extend across thousands of degrees of freedom. For example, the initial factorization of the dynamic coefficient matrix for a model with 5000 structural and 250 fluid equations (a typical mix) would require roughly 3 hrs of CPU time on the CDC 6600 computer.

1.2 STAGGERED SOLUTION PROCEDURE

The staggered solution scheme consists of splitting the time integration task between two loosely coupled processors, a fluid and a structural analyzer, with the interaction effects being incorporated through an extrapolation mechanism. If certain practical restrictions (described in the body of the paper) are met, this strategy offers the important advantage of preserved program modularity, in the sense that the organization of the structural time integration package is not sensibly affected. A general-purpose fluid analyzer may be developed and checked out as independent of any specific structural code and eventually "plugged in" as a modular component to interface with any large-scale structural analyzer. Furthermore, subsequent improvements made in the fluid analyzer will be essentially transparent to the user, resulting in corresponding gains in efficiency. Additional advantages accruing in the treatment of nonlinear structural response problems are discussed in the section on implementation.

Given the usual proportion of structural to fluid equations (4:1 through 25:1 in three-dimensional problems), the bulk of the computational effort is most likely to fall upon the structural analyzer, which perceives the fluid only as an external force environment. It is therefore reasonable to expect that the fluid-structure problem can be processed for only a marginal increment in the cost required for processing the "dry" structure only (provided, of course, that similar time increments and structural solution strategies are used in both cases). The price paid for these computational advantages is the fact that satisfactory numerical stability characteristics are much harder to achieve for the staggered procedure. No such difficulties arise in the pressure-elimination or simultaneous solution procedures, for which the selection of one of the many available A-stable time integration operators suffices to secure unconditional stability.

The purpose of this report is to examine the fundamental algorithmic properties -- convergence, stability and accuracy -- of the staggered solution procedure when the fluid-structure interaction is treated by the DAA. It will be shown that the simplest (conventional) formulation of the staggered procedure for the structure/DAA equations suffers from severe time-increment limitations due to stability considerations. Such restrictions effectively rule out the use of the conventional staggered solution procedure as a general-purpose method, although that scheme can work satisfactorily in a restricted class of shock-excited problems.

The main objective of this investigation is to find ways to extend the range of applicability of the staggered solution procedure. It happens that a satisfactory stabilization of that strategy can be achieved by a judicious modification of the original equations of motion through a process of augmentation. There are a number of ways in which the fluid and/or the structural equations can be augmented to produce the desired stabilization, but only one survives if the practical constraint of limiting modifications to existing structural analyzers is imposed.

1.3 OUTLINE OF THIS REPORT

In the section following, equations of motion that govern a spatially-discretized, fluid-structure interaction problem treated by the DAA are introduced. An associated two degree-of-freedom system is derived and converted to dimensionless coordinates. This system is time-discretized through application of linear multistep operators and the resulting integration process is expressed in the conventional staggered solution form. A study of the domain of convergence of the iterated process and of the temporal stability characteristics shows that this formulation has a limited applicability range because of time-increment limitations.

The source of instability of the conventional staggered procedure is then explored in detail. This investigation is carried out by using a time-delayed continuous form of the extrapolated coupling term (predictor) for deriving a difference-differential system. Examination of the characteristic equation of this system clearly shows that the onset of instability is caused by the delayed feedback of fluid radiation damping from the fluid equation into the structural equation. This result leads us to consider the use of "damping augmentation" strategies that are often employed in the field of control theory to stabilize systems with dead-time (delay) elements.

Several stabilized formulations are then developed by tailoring the governing equations of motion in such a way that appropriate damping terms appear in the structural equations, the fluid equations, or both. A study of the iterative convergence and temporal stability of these forms show that they are globally convergent and remain unconditionally stable for certain extrapolators.

An extensive series of numerical experiments has been conducted with the dual objective of verifying the predictions of the stability analysis and of assessing the global accuracy of the computed solutions of the two degree-of-freedom system. Representative results of this series are presented. Practical considerations regarding the computer implementation of the stabilized formulations to treat large-scale problems are then offered; special emphasis is placed on software modularity requirements. Finally, the main conclusions derived from the present investigation are summarized.

SECTION II

GOVERNING EQUATIONS

Consider a structure interacting with an acoustic medium through a contact boundary B, henceforth referred to as the "wet surface." The structure and fluid are spatially discretized through the application of finite-element and boundary-integral techniques, respectively. (It is important to note that the corresponding meshes on B are not necessarily identical.) The resulting matrix equations of motion may be written as

$$\begin{aligned} \underset{\sim}{M}\,\underline{\ddot{u}} + \underset{\sim}{D}\,\underline{\dot{u}} + \underset{\sim}{K}\,\underline{u} &= \underline{f}_s + \underline{r} - \underset{\sim}{T}\,\underset{\sim}{A}\,(\underline{p}^S + \underline{p}^I) \\ \underset{\sim}{M}_f\,\dot{\underline{q}} + \rho\, c\, \underset{\sim}{A}\,\underline{q} &= \rho\, c\, \underset{\sim}{M}_f\,(\underset{\sim}{T}^T\,\underline{\dot{u}} - \underline{\dot{u}}^I) \end{aligned} \tag{1}$$

where the first set of equations expresses dynamic equilibrium in terms of the structural displacements, and the second set, the DAA, describes the fluid-structure interaction at the wet surface. (Recall that the number of structural equations is usually much greater than the number of fluid equations.) In (1), $\underset{\sim}{M}$, $\underset{\sim}{D}$, and $\underset{\sim}{K}$ are the structural mass, damping and linear (or linearized) stiffness matrices, respectively; $\underline{u}$, $\underline{f}_s$ and $\underline{r}$ are the structure response displacements, dry-structure applied force, and nonlinear residual (pseudo-force) vectors, respectively; $\underline{p}^S = \dot{\underline{q}}$ is the scattered pressure vector and $\underline{p}^I$ is the incident pressure vector, appropriate to the fluid grid on B; $\underset{\sim}{A}$ is a diagonal matrix embodying elemental areas of the fluid mesh on the wet surface B, $\underset{\sim}{M}_f$ is the fluid mass matrix as determined from an analysis of incompressible fluid motion appropriate to a distribution of elemental sources on B, $\underset{\sim}{T}$ is a generally rectangular transformation matrix that relates structural displacements to the control points of the fluid grid on B, ρ and c are fluid density and speed of sound, respectively, and superscript T denotes matrix transposition; finally, the superscript dot ($\dot{}$) denotes temporal differentiation.

2.1 THE MODEL PROBLEM

The homogeneous linear (or linearized) part of (1) can be expressed as

$$\begin{bmatrix} \underset{\sim}{M} & \underset{\sim}{0} \\ \underset{\sim}{0} & \underset{\sim}{0} \end{bmatrix} \begin{Bmatrix} \underline{\ddot{u}} \\ \ddot{\underline{q}} \end{Bmatrix} + \begin{bmatrix} \underset{\sim}{D} & \underset{\sim}{T}\underset{\sim}{A} \\ \rho c \underset{\sim}{M}_f \underset{\sim}{T}^T & \underset{\sim}{M}_f \end{bmatrix} \begin{Bmatrix} \underline{\dot{u}} \\ \dot{\underline{q}} \end{Bmatrix} + \begin{bmatrix} \underset{\sim}{K} & \underset{\sim}{0} \\ \underset{\sim}{0} & \rho\, c \underset{\sim}{A} \end{bmatrix} \begin{Bmatrix} \underline{u} \\ \underline{q} \end{Bmatrix} = \begin{Bmatrix} \underline{0} \\ \underline{0} \end{Bmatrix} \tag{2}$$

In the following study, the structural damping term $\underset{\sim}{D}\,\underline{\dot{u}}$ will be systematically neglected, as its effect on the response is in most cases negligible when compared to that of the fluid radiation damping term $\underset{\sim}{T}\underset{\sim}{A}\dot{\underline{q}}$. An appropriate two degree-of-freedom problem associated with the system (2), after setting $\underset{\sim}{D} = \underset{\sim}{0}$, is

$$m_s \ddot{w} + k_s w = - a \dot{g}$$

$$m_f \dot{g} + \rho c a g = \rho c m_f \dot{w} \tag{3}$$

where m_s, k_s, a and m_f are generalized quantities resulting from the projection of $\underset{\sim}{M}$, $\underset{\sim}{K}$, $\underset{\sim}{A}$ and $\underset{\sim}{M}_f$, respectively, on normal coordinates w and g that diagonalize the left-hand side of (2). The derivation of (3) is presented in Appendix A. We note that (3a) represents a pressure-excited undamped mechanical oscillator whereas (3b) represents a velocity-excited pressure-decay equation.

The system (3) can be further reduced to the non-dimensional form

$$\xi \ddot{x} + \omega^2 x = - \dot{y}$$

$$\dot{y} + \mu y = \dot{x} \tag{4}$$

through introduction of the dimensionless variables

$$x = w/\ell \quad , \quad y = g/(\rho c \ell)$$

$$\xi = m_s/(\rho \ell a) \quad , \quad \omega^2 = k_s \ell^2/(\xi m_s c^2)$$

$$\mu = m_s/(\xi m_f) = \rho \ell a/m_f \tag{5}$$

$$(\dot{}) = \partial/\partial\tau \quad , \quad \tau = c\,t/\ell$$

In Eqs. (5), ℓ denotes a characteristic length of the problem, e.g., the radius of a submerged cylinder or sphere; ξ is a "buoyancy ratio" (structural mass divided by displaced fluid mass), ω is a reduced vibration frequency, and μ is a generalized-pressure decay exponent. Note that the dot superscript has been redefined in (5d) to denote differentiation with respect to the dimensionless time τ, rather than physical time t.

2.2 TEMPORAL DISCRETIZATION

We shall consider the use of implicit, one-derivative linear multistep (LMS) methods to effect the time discretization of (4). For a constant step-size $h = \Delta\tau$, an m-step method can be presented in the compact form

$$z_n = \delta\, \dot{z}_n + h_n^z \tag{6}$$

where z stands for a scalar or vector state variable, the subscript n is the time station index, δ is the generalized time step βh (β being a method coefficient), and the historical vector h_n^z is a linear combination of m past solutions:

$$h_n^z = -\sum_{i=1}^{m} (\alpha_i\, z_{n-i} - \beta_i\, h\, \dot{z}_{n-i}) \tag{7}$$

Specific LMS integrators are characterized by the coefficients β, α_i and β_i. For example, the trapezoidal rule ($m = 1$) has $\alpha_1 = -1$, $\beta = \beta_1 = 0.5$.

For reasons to be justified later, we introduce a <u>pair</u> of LMS integrators

$$\begin{aligned} x_n &= \delta_x x_n + h_n^x\,, \quad \delta_x = \beta_x h \\ y_n &= \delta_y y_n + h_n^y\,, \quad \delta_y = \beta_y h \end{aligned} \tag{8}$$

to treat the reduced equations (4). The resulting algebraic system is

$$\begin{aligned} (\xi + \delta_x^2 \omega^2)\, x_n &= -\delta_x^2 \dot{y}_n + \xi\, (h_n^x + \delta_x h_n^{\dot{x}}) \\ (1 + \delta_y\, \mu)\, \dot{y}_n &= \dot{x}_n - \mu\, h_n^y \end{aligned} \tag{9}$$

The secondary state variables, velocity $\dot{x}_n$ and pressure integral y_n, are calculated from the integrators (8), *i.e.*

$$\begin{aligned} \dot{x}_n &= (x_n - h_n^x)/\delta_x \\ y_n &= h_n^y + \delta_y\, \dot{y}_n \end{aligned} \tag{10}$$

Eqs. (9) and (10) form the basis for the analysis of the conventional staggered solution procedure.

2.3 RANGE OF NON-DIMENSIONAL PARAMETERS

The time-discretized system (9) contains four non-dimensional parameters: ξ , ω , μ and h . The first three embody spatial characteristics of the problem whereas h introduces the effect of the time integration stepsize. It is of interest to the forthcoming discussions on the applicability of various implementations of the staggered procedure, to exhibit typical ranges assumed by such quantities. This information is collected in Table 1.

For ξ , ω , and μ , two limit conditions and an illustrative case are shown. The cavity condition is the limit of modal motions heavily dominated by the inertia of the fluid, viz. low-frequency motions of a very thin submerged shell. The dry mode condition is realized by structural motions that do not interact with the fluid, such as torsional modes of structures of revolution. The illustrative problem of a submerged spherical shell is of interest because this is one of the few geometries amenable to exact analytical modal treatment, as discussed in Appendix B. Ranges quoted for the dimensionless time increment $h = c\Delta t/\ell$ are tabulated according to the temporal characteristics of the excitation, which determines the energy-spectrum characteristics of the response.

TABLE 1. Range of Non-Dimensional Parameters

Parameter	Limit Cases		Illustrative Case
	Cavity $m_s \to 0$, $k_s \to 0$	Dry Structural Mode $m_f \to 0$, $a \to 0$	Submerged Spherical Shell[a]
ω	0[b]	≥ 0	0 to $\sim \bar{\rho}\bar{c}e^{\frac{1}{2}} n^2$
ξ	0	∞	$\sim \bar{\rho}e$ to $\sim \bar{\rho}en^2$
μ	1	indet.	1 to n + 1
	Shock-Excited Problems[c] Early-Time[d] Response / Late-Time[e] Response		Structural Dynamics Problems[f]
h	0.01-0.1	1-100	>>1

[a] $\bar{\rho} = \rho_s/\rho$ = ratio of shell and fluid densities, $\bar{c} = c_s/c$ = ratio of sound speeds in shell and fluid, e = thickness-to-radius ratio, n ≅ highest circumferential wave number retained. These equations are derived in Appendix B, where numerical values of ω, ξ and μ are tabulated for a particular combination of $\bar{\rho}$, $\bar{c}$ and e.

[b] k_s tends to zero faster than m_s.

[c] Problems characterized by wave propagation effects.

[d] Period during which shock wave starts to envelop the structure ($\tau < 1$); characterized by high-frequency structural motions, high radiation damping, relatively small hydrodynamic inertia forces.

[e] Period characterized by low-frequency structural motions, dominant hydrodynamic inertia, and low radiation damping (usually $\tau \gtrsim 10$).

[f] Problems characterized by low-frequency motions throughout.

SECTION III

PRESSURE EXTRAPOLATION FORMULATION

The simplest formulation of the staggered scheme suggested by the format of Eqs. (9), is the pressure extrapolation (PE) formulation, which may be described as follows. Assume that solutions up to the (n-1)th time station are known. We first predict the pressure $\dot{y}_n^P$ at t_n, insert this into the right-hand side of (9a), solve for the structural displacement x_n, obtain the velocity $\dot{x}_n$ from (10a), insert this into (10b) and finally solve for the pressure $\dot{y}_n$. This corrected value may be used in an iterative setting if desired. We proceed now to analyze the iteration convergence and temporal stability properties of the PE formulation.

3.1 ITERATION CONVERGENCE

Using k as an iteration cycle index, the iterated PE scheme may be written

$$\left.\begin{aligned} E_x\, x_n^{(k)} &= -\beta_x\, h\chi\, \dot{y}_n^{(k-1)} + b_x \\ E_y\, \dot{y}_n^{(k)} &= (x_n^{(k)} - h_n^x)/\delta_x + b_y \end{aligned}\right\} \quad k = 1,2 \ldots \tag{11}$$

where

$$\begin{aligned} E_x &= 1 + \beta_x^2\, \Omega^2\,, \quad \Omega^2 = \omega^2\, h^2/\xi \\ E_y &= 1 + \beta_y\, \Psi\,, \quad \Psi = \mu\, h \\ \chi &= h/\xi \\ b_x &= h_n^x + \delta_x\, h_n^{\dot{x}}\,, \quad b_y = -\mu\, h_n^y \end{aligned} \tag{12}$$

The initial $\dot{y}_n^{(0)} = \dot{y}_n^P$ may be obtained from a simple predictor such as

$$\dot{y}_n^{(0)} = (1 + \gamma)\ \dot{y}_{n-1} - \gamma\, \dot{y}_{n-2} \tag{13}$$

where γ is an extrapolation parameter (actually, extrapolation corresponds to $\gamma > 0$. and interpolation to $\gamma \le 0$).

The iterative scheme (11) can be recast into the standard form

$$\underline{z}^{(k)} = \underset{\sim}{R}\, \underline{z}^{(k-1)} + \underline{b} \tag{14}$$

where $\underline{z}^T = (x_n, \dot{y}_n)$, $\underline{b}$ embodies terms independent of k, and the iteration matrix $\underset{\sim}{R}$ is

$$\underset{\sim}{R} = \begin{bmatrix} E_x & 0 \\ 1 & E_y \end{bmatrix}^{-1} \begin{bmatrix} 0 & \beta_x h\chi \\ 0 & 0 \end{bmatrix} = \frac{\beta_x h\chi}{E_x E_y} \begin{bmatrix} 0 & E_y \\ 0 & 1 \end{bmatrix} \tag{15}$$

The iteration (14) converges if and only if the spectral radius κ of $\underset{\sim}{R}$ (largest eigenvalue modulus) is less than 1. Since $\kappa(\underset{\sim}{R}) = \beta_x \chi/(E_x E_y)$, the convergence condition is

$$\chi = h/\xi < (1 + \beta_x \Omega^2)(1 + \beta_y \Psi)/\beta_x \tag{16}$$

The right-hand side of (16) is minimized for modal motions with $\Omega \to 0$, $\Psi \to 0$, in which reads

$$\chi < 1/\beta_x \tag{17}$$

The structural equations will normally be treated with an A-stable integrator to account for the wide frequency spectrum present in most discrete models. But for all A-stable LMS methods, β_x lies in the range of ½ to 1. Consequently,

$$\chi = h/\xi < 2.0 \tag{18}$$

is the best that can be achieved by using the trapezoidal rule ($\beta_x = ½$) in (8). Note that the convergence conditions are not only independent of the pressure predictor (as one would expect of a linear system), but of the historic term composition of the integrator pair (8) as well.

3.2 TEMPORAL STABILITY

The numerical stability of the PE formulation has been studied for a variety of LMS integrators, assuming the two-step predictor (13), and a fixed number (k) of passes per time step. No details of the analysis will be given here, inasmuch as the conventional staggered procedure is not recommended for general use. Only one illustrative example and some general observations will be offered.

The stability region of the PE formulation is always χ-bounded, i.e., parameters ω and μ play no role in the analysis (in more precise terms, the worst combination is $\omega = \mu = 0$), and neither does the fluid integrator (8b). For a specific structural integrator (8a) and the one-parameter predictor (13), the stability regions can be conveniently

displayed in the (γ,χ) plane. Figure 1 shows those curves for the trapezoidal rule. The largest stable χ is 4, which can be attained for the one-pass solution $(k = 1)$ if $\gamma = -\frac{1}{2}$ (the predicted pressure value is the mean of the last two values). If the process is iterated, the peak of the stability region is reduced; and as $k \to \infty$ the stability limit approaches the predictor-independent value (18).

It should be stressed that a time increment limited by a $\chi = h/\xi$ of order 2 to 4 is unacceptable for a general-purpose integration package. The constraint can be practically met only in a limited class of problems, such as the early-time shock response of submerged structures. If the response is dominated by low-frequency structural motions, however, that increment limit is intolerably small; so small, in fact, that computational error accumulation and computation time become critical. (The largest stable χ found by the authors is 8, which requires the implementation of a fairly elaborate time-advancement procedure.)

3.3 OBSERVATIONS

The detailed study of the range of convergence of the iterated PE formulation can be justified by the following considerations. Suppose we had found that the iteration (11) converges for the entire range (or at least a wide range) of parameters. The converged solution $x_n^{(\infty)}$, $\dot{y}_n^{(\infty)}$ would then be identical to that furnished by the fully-implicit scheme resulting

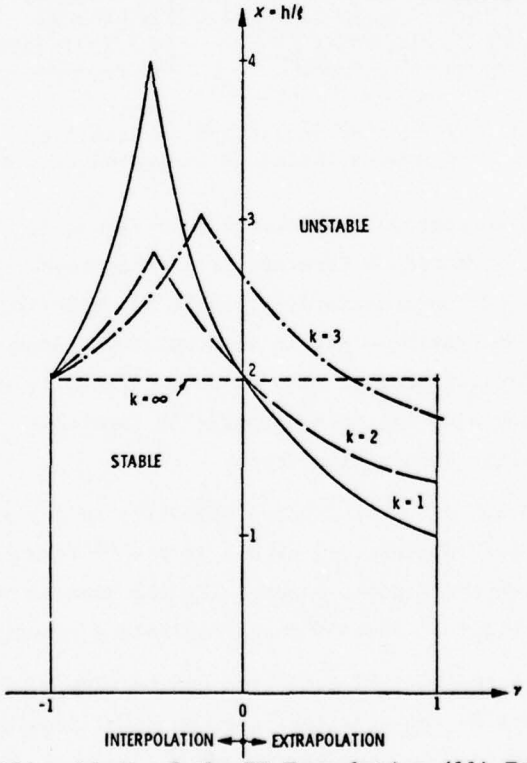

Figure 1 Stability Limit of the PE Formulation (11) Treated by the Trapezoidal Rule and the Two-Step Predictor (13) as a Function of the Number of Passes (k) per Time Step

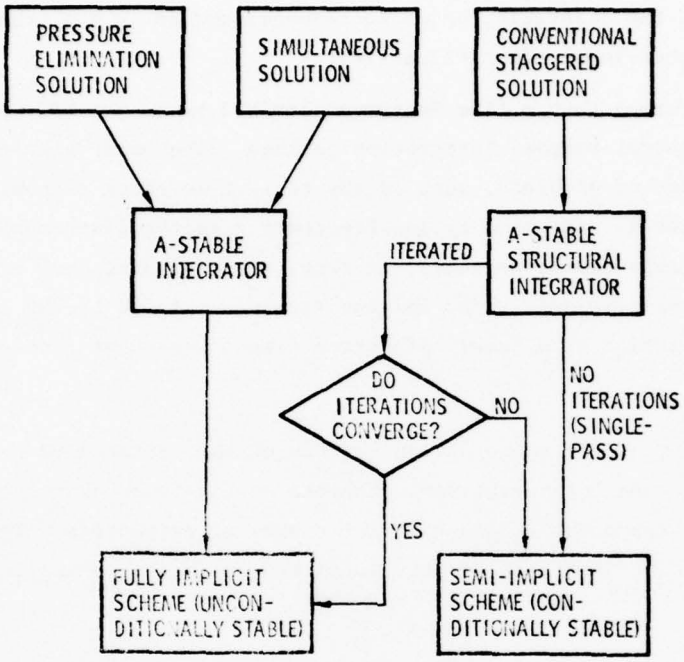

Figure 2 Effect of Iterations on Stability Characteristics of Staggered Procedures

from the simultaneous solution approach, as sketched in Figure 2. Under such assuptions, the stability region of the iterated PE formulation must approach that of the fully-implicit scheme. The latter can be made unconditionally stable by selecting a suitable A-stable LMS method. Iteration would then provide a simple strategy for transmuting the one-pass, conditionally stable semi-implicit procedure into an unconditionally stable scheme of greater accuracy; this strategy might have led to a potentially favorable tradeoff between iteration cost and the ability to utilize larger time steps.

As increasing k does not actually improve stability to any significant extent, it appears that there is no point in iterating at all if the PE formulation is used. (In linear problems, an iteration cycle costs essentially the same as one advancing step, but higher accuracy can be generally achieved through equivalent reductions in the stepsize.)

Finally, it should be noted that PE iteration can be made to converge over the entire feasible domain of parameters by the application of a Jacobi acceleration strategy [4,§ 4.3.1] to (11). The resulting iteration process is virtually identical, however, to those ensuing from stabilization of the original equations (4) by augmentation, as described in later sections.

3.4 VELOCITY EXTRAPOLATION PROCEDURE

An alternative formulation of the conventional staggered solution procedure can be based on velocity extrapolation (VE) applied to the fluid equation (9b). The algorithmic properties of this formulation are identical to those of the PE formulation, and need not be discussed further.

SECTION IV

SOURCE OF INSTABILITY

This section probes more deeply into the underlying causes of the iteration divergence and temporal stability limitations exhibited by the conventional (PE, VE) formulation of the staggered solution procedure. First we examine the root locus diagram of the characteristic equation pertaining to the fully-implicit formulation of the model system (4), noting its essentially stable character. The PE solution procedure is then cast into a differential-difference (DD) system that abstracts the time integration method. The analysis of the characteristic equation of the DD system shows clearly that the χ-limited instability is, as expected, caused by the feedback effect of the extrapolated pressure term into the structural equations of motion. This analysis technique has the important advantage of providing results that are independent of the intrusion of a particular time integration scheme; the effect of the latter is, in fact, of secondary importance. Interpretation of the results in terms of a control process provides direct insight into techniques for the stabilization of the staggered solution procedure at the differential equation level; such techniques are exploited in the following section.

4.1 CHARACTERISTICS OF THE FULLY-IMPLICIT FORMULATION

We obtain the homogeneous form of the fully-implicit model system by transferring the coupling terms in (4) to the left-hand sides, which yields

$$\begin{aligned} \xi\,\ddot{x} + \dot{y} + \omega^2 x &= 0 \\ \dot{y} - \dot{x} + \mu y &= 0 \end{aligned} \tag{19}$$

Laplace transformation of these equations without consideration of initial conditions then yields

$$\begin{bmatrix} \xi s^2 + \omega^2 & s \\ -s & s + \mu \end{bmatrix} \begin{Bmatrix} X(s) \\ Y(s) \end{Bmatrix} = \underline{0} \tag{20}$$

in which $X(s)$ and $Y(s)$ denote the transforms of $x(t)$ and $y(t)$, respectively. The associated characteristic equation is therefore

$$(\xi s^2 + \omega^2)(s + \mu) + s^2 = 0 \tag{21}$$

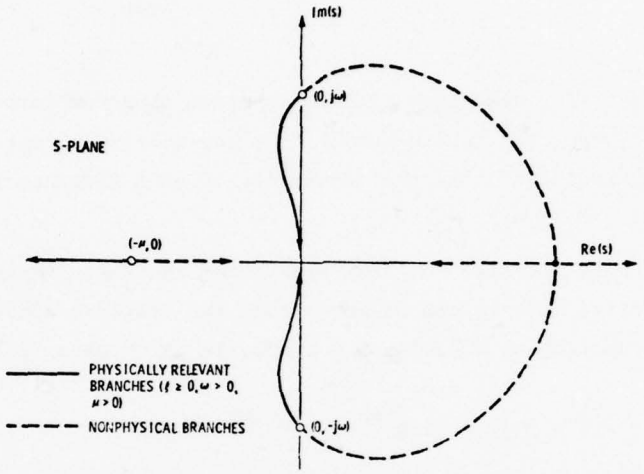

Figure 3 Root Locus Diagram of the Fully-Implicit System (19) in the Laplace-Transform-Variable Space

The root locus diagram for (21) is shown in Figure 3. Because all physically relevant branches are on the left-hand side ($\mathrm{Re}(s) \leq 0$, (19) are inherently stable equations. Consequently, a stable numerical solution is guaranteed if the time integrator applied to (19) is A-stable.

4.2 CHARACTERISTICS OF THE PE FORMULATION

A differential-difference (DD) equation [5] for the PE formulation can be obtained by expressing the two-step predictor (13) in a delayed continuous form,

$$\dot{y}^P(t) = (1 + \gamma)\, \dot{y}(t - h) - \gamma\, \dot{y}(t - 2h) \tag{22}$$

This form is applied to the model system (4) to obtain

$$\begin{aligned} \xi\, \ddot{x}(t) + \omega^2\, x(t) &= -(1 + \gamma)\, \dot{y}(t - h) + \gamma\, \dot{y}(t - 2h) \\ \dot{y}(t) + \mu\, y(t) &= \dot{x}(t) \end{aligned} \tag{23}$$

which is the DD form associated with the single-pass PE formulation. Note that (23) is independent of any time integration scheme. Its characteristic equation in the Laplace-transform variable s is obtained following a procedure identical to that used to obtain (21):

$$(\xi\, s^2 + \omega^2)\,(s + \mu) + s^2\,[(1 + \gamma)\, e^{-sh} - \gamma\, e^{-2sh}] = 0 \tag{24}$$

In control theory, the identifier dead-time element is often used for terms such as e^{-sh} and e^{-2sh} (see, e.g., [6], p. 284), which result from Laplace-transormation of time-delayed terms. It is generally acknowledged that the occurrence of such elements in control loops has a destabilizing effect.

In the limit of vanishing stepsize h, (24) approaches the fully implicit equation (21), which is stable. For a finite h, it can be shown that the critical combination of parameters pertaining to the stability of (24) is $\omega = \mu = 0$, in which case (24) reduces to

$$\xi\, s + (1 + \gamma)\, e^{-sh} - \gamma\, e^{-2sh} = 0 \tag{25}$$

Equation (25) shows that stability is characterized in terms of three parameters: the "buoyancy ratio" ξ, the dead-time constant h (integration stepsize), and the extrapolation parameter γ. The critical component is, of course, h, which can be viewed, from the DD-form standpoint, as the sampling rate with which pressures are evaluated and fed back into the structural analyzer by the extrapolator (22). The destabilizing effect of the dead-time element can be investigated by recasting (25) in the form

$$1 + G(s) = 0 \tag{26}$$

where

$$G(s) = \frac{1}{\xi\, s}\,[(1 + \gamma)\, e^{-sh} - \gamma\, e^{-2sh}] \tag{27}$$

The most expedient approach for investigating the existence of unstable roots $\mathrm{Re}(s) > 0$ of a complex transcendental equation such as (26) is due to Nyquist [7]. For the special form (26), Nyquist's criterion can be stated as follows: let the Laplace-transform variable s encircle the entire right-hand plane $\mathrm{Re}(s) > 0$ by varying $s = j\,v$ ($j^2 = -1$) from $v = -\infty$ to $+\infty$, and find the angle of $G(jv)$ in the polar coordinate system $[|G(s)|\ ,\ \measuredangle\, G(s)]$ that satisfies

$$\measuredangle\, G(s) = \pi\ ,\ |G(s)| \leq 1 \tag{28}$$

Application of this criterion to (27) provides the two conditions

$$(1 + \gamma) \cos \nu h - \gamma \cos 2\nu h = 0$$

$$\xi \nu h/h \geq (1 + \gamma) \sin \nu h - \gamma \sin 2\nu h \tag{29}$$

For the special case $\gamma = 0$, i.e., using the last pressure solution as the predicted value, (29) gives the stability limit

$$\chi = h/\xi \leq \pi/2 \tag{30}$$

Figure 4 shows the stability limit in the (χ, γ) plane as calculated from (29). The destabilizing effect of the dead-time element is now apparent. It must be stressed again that the stability boundary shown in Figure 4 applies only if an integration scheme of infinite accuracy (such as an analytical integration or a nontruncated Taylor series algorithm) is used to solve the system (23), and that the boundary is perturbed by the intrusion of a difference time integrator. For example, the use of the trapezoidal rule as the structural integrator increases the stability domain, as can be deduced from a comparison of Figures 1

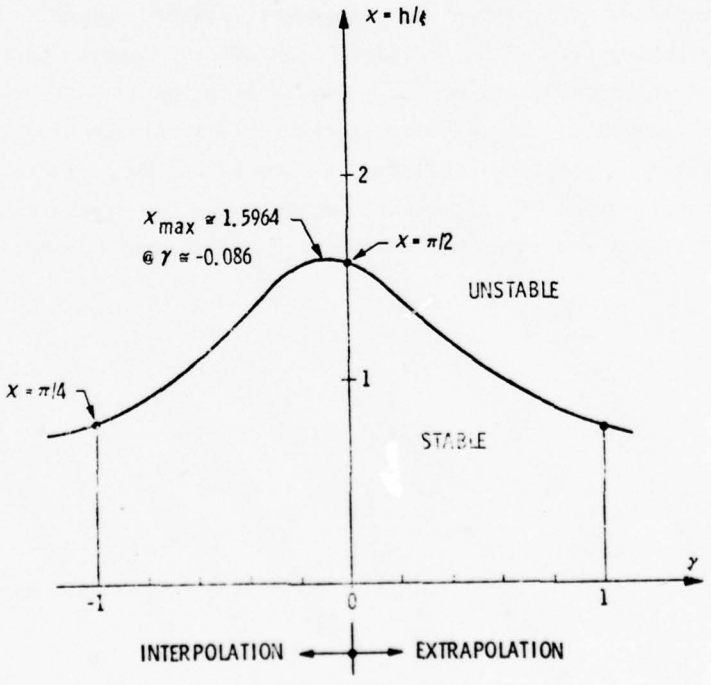

Figure 4 Stability Limit of the Difference-Differential Form (24) of the PE Formulation with the Two-Step Predictor (22)

and 4; on the other hand, the use of the backward Euler method (not shown here) has a detrimental effect on stability.

4.3 SUMMARY OF MAIN FINDINGS

- The χ-bounded stability of the conventional (PE, VE) procedure is due to the dead-time (delayed) pressure feedback (22) into the structural equations (23). This process can be viewed (in control theory terms) as a sampled-feedback system, in which the pressure feedback is delayed by a "hold" (dead-time interval) equivalent to the stepsize h. This representation is illustrated in the block diagram of Figure 5.

- The most commonly used strategy for stabilization of a system that includes dead-time components consists of introducing a series of compensating elements that reduce the bandwidth of the system's frequency response (see, e.g., [8] p. 118). These stabilization techniques essentially amount to the introduction of damping into the feedback loop.

- In the fully-implicit solution procedure, damping is inherently present by virtue of the energy radiation term $(\dot{y})$ in the model system (19) on the left-hand side. The effect of the radiation damping on the structural response roots can be readily appreciated by examining Figure 3. The structural equation (23) of the PE procedure, however, contains no homogeneous damping term. The addition of artificial damping to the structural equation (23a) and/or the pressure equation (23b) in amounts sufficient to stabilize the solution procedure is likely to have catastrophic effects on solution accuracy. We are therefore motivated to attempt the restoration of sufficient damping to achieve overall stability through appropriate rearrangement of the original governing equations.

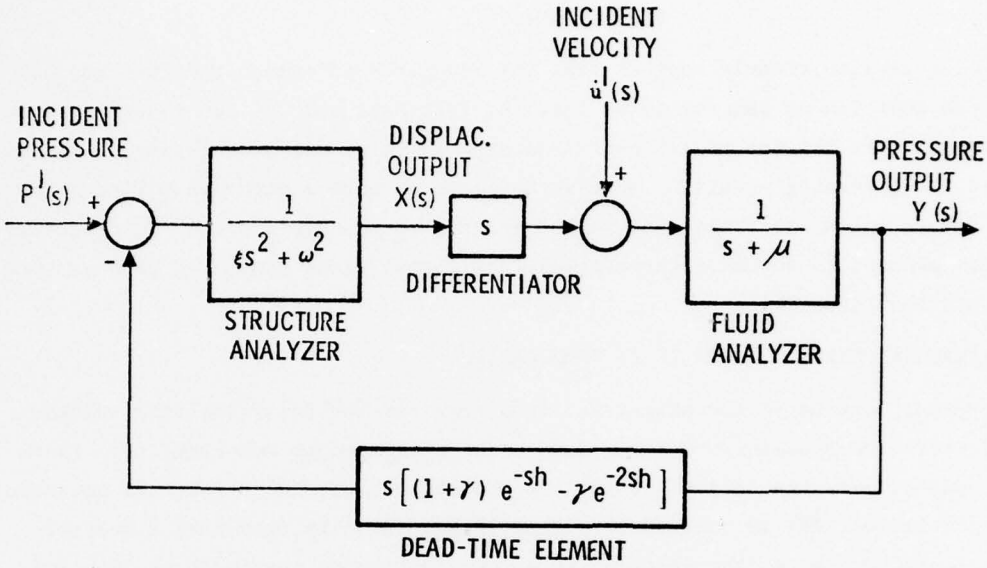

Figure 5 Control Loop Representation of the Pressure Extrapolation Procedure (24)

SECTION V

STABILIZATION

The foregoing results clearly suggest that the staggered solution procedure may be stabilized by the addition of damping terms into the left-hand side of the governing equations of motion. As the use of artificial damping is ruled out by accuracy considerations, it follows that the governing equations must be tailored in such a way that homogeneous damping terms either appear in the structural equations, or be added to the fluid equations, or both. We now proceed to describe three stabilized formulations generated through such "damping augmentation" techniques.

5.1 PRESSURE-INTEGRAL EXTRAPOLATION (PIE) FORMULATION

The homogeneous portion of the structural equations for the fully-implicit solution procedure (19) effectively exhibits damping due to the simultaneous velocity $(\dot{x})$ feedback from the coupled pressure equation (19). On the other hand, the structural equation for the PE formulation (23) is excited by a time-lagged velocity feedback; a destabilizing effect occurs because of the delayed energy dissipation in the feedback loop (cf. Figure 5). We can correct this situation by eliminating the time-lagged velocity feedback; this is accomplished mathematically by combining (4a) and (4b):

$$\xi \ddot{x} + \omega^2 x = -\dot{y} = -(\dot{x} - \mu y) \tag{31}$$

which, upon transferring the damping term $(\dot{x})$ to the left-hand side, becomes

$$\xi \ddot{x} + \dot{x} + \omega^2 x = \mu y \tag{32}$$

The solution procedure based upon (32) along with the original pressure equation (4b) will be called the pressure-integral extrapolation (PIE) formulation, inasmuch as the pressure-integral y is involved in the prediction process.

5.2 DISPLACEMENT EXTRAPOLATION (DE) FORMULATION

Stabilization can also be achieved by augmentation of the fluid equation so as to increase the pressure decay rate in the homogeneous system. Qualitatively speaking, this strategy works as long as the stability "margin" of the modified pressure equation overwhelms the destabilizing effect of the structural equations. The modified pressure equation is obtained by the substitution of (4a) into the time-differentiated (4b):

$$\ddot{y} + \mu \dot{y} = \ddot{x} = -(\dot{y} + \omega^2 x)/\xi \tag{33}$$

which can be rearranged to form

$$\ddot{y} + (\mu + 1/\xi)\, \dot{y} = -\omega^2\, x/\xi \tag{34}$$

The solution procedure based upon (34) along with the original structural equation (4a) will be called the displacement extrapolation (DE) formulation.

5.3 OTHER FORMULATIONS

The three formulations of the model problem described so far are collected in Table 2. It turns out that additional, more complicated, formulations may be constructed. As these have not been found to possess any particular advantage over the two preceding formulations, they will not be discussed here.

TABLE 2. Model Formulations for Staggered Solution Procedures

Formulation	Model Equations	Extrapolated Quantity
Pressure Extrapolation (PE)	$\xi\, \ddot{x} + \omega^2\, x = -\dot{y}$ $y + \mu\, y = x$	$\dot{y}$
Pressure-Integral Extrapolation (PIE)	$\xi\, \ddot{x} + \dot{x} + \omega^2\, x = \mu\, y$ $\dot{y} + \mu\, y = \dot{x}$	y
Displacement Extrapolation (DE)	$\xi\, \ddot{x} + \omega^2\, x = -\dot{y}$ $\ddot{y} + (\frac{1}{5} + \mu)\, \dot{y} = -\frac{\omega^2}{\xi}\, x$	x

SECTION VI

ITERATION CONVERGENCE OF STABILIZED FORMULATIONS

The iteration convergence properties of the stabilized formulations derived in the foregoing section may be studied with a technique similar to that used to analyze the iterated PE scheme (11). The convergence conditions are collected in Table 3.

It is easily shown that the spectral radii for the two augmented schemes are less than unity over the entire feasible domain (0 to $+\infty$) of the parameters χ, Ω and Ψ. The key significance of this result is: if the solution is iterated to convergence at each time step, the solution of the fully-implicit scheme is recovered (cf. Figure 2). With such convergence guaranteed, we have now at our disposal a feasible computational strategy by which unconditional stability can be attained within the basic organization of the staggered solution procedure.

TABLE 3. Iteration Convergence Characteristics of Staggered Solution Procedures

Formulation	Spectral Radius, κ, of Iteration Matrix Iteration converges if $\kappa < 1$.
PE	$\beta_x \chi / [(1 + \beta_x^2 \Omega^2)(1 + \beta_y \Psi)]$
PIE	$\beta_y \beta_x \chi \Psi / [(1 + \beta_y \Psi)(1 + \beta_x \chi + \beta_x^2 \Omega^2)]$
DE	$\beta_y \beta_x^2 \chi \Omega^2 / [(1 + \beta_y \Psi + \beta_y \chi)(1 + \beta_x^2 \Omega^2)]$

6.1 SELECTION OF A PREDICTOR

A wide variety of predictor formulas can be used in the practical implementation of the stabilized procedures. The ideal formula should be able to provide satisfactory extrapolation accuracy for physically meaningful response components without jeopardizing the temporal stability characteristics; this is indeed a delicate compromise. The following considerations are aimed at restricting the class of admissible formulas to predictors that exclude "historical derivatives". A predictor that includes derivatives of past solutions introduces large extrapolation errors in both high-frequency structural response components ($\Omega >> 1$) and rapidly-decaying pressure response components ($\Psi >> 1$). Table 3 shows that, as either $\chi \Psi$ or $\chi \Omega^2$ becomes large, the corresponding spectral radii approach unity. On the other hand, for low-frequency components, i.e., as either χ or Ψ and/or Ω tend to zero, all spectral radii approach zero. This means that extrapolation errors committed for "noise" components of the response (i.e., those with large Ψ and/or Ω) will decrease very slowly with increasing iteration index.

We therefore restrict our considerations to predictors that are less prone to "excite" noise components. The following three-step, two-parameter family can be considered sufficient for our envisioned applications:

$$z_n^P = [(1 + \gamma_1)(1 - \gamma_2) + 3\gamma_2] z_{n-1} - [(1 - \gamma_2)\gamma_1 + 3\gamma_2] z_{n-2} + \gamma_2 z_{n-3}$$

where z stands for the solution-state term being extrapolated. Special cases of (35) are listed in Table 4.

6.2 SINGLE-PASS STABILIZED PROCEDURES

The difference equations for the single-pass PIE formulation are [cf. (T2)]

$$\begin{aligned} E_x x_n^{(1)} &= \beta_x^2 \chi \Psi y_n^{(0)} + (1 + \beta_x \chi) h_n^x + \beta_x h h_n^{\dot{x}} \\ E_y y_n^{(1)} &= \beta_y (x_n^{(1)} - h_n^x)/\beta_x + h_n^y \end{aligned} \tag{36}$$

where $y_n^{(0)}$ is predicted by means of (35),

$$E_x = 1 + \beta_x \chi + \beta_x^2 \Omega^2 \tag{37}$$

TABLE 4. Predictors Considered for the Present Study

Case	Parameters	Order of Accuracy
I	$\gamma_1 = \gamma_2 = 0$	Zero order
II	$\gamma_1 = 1/2$, $\gamma_2 = 0$	Improved zero-order
III	$\gamma_1 = 1$, $\gamma_2 = 0$	First order
IV	$\gamma_1 = 1$, $\gamma_2 = 1/2$	Improved first order[a]
V	$\gamma_1 = 1$, $\gamma_2 = -2/3$	Lease-square fit

[a]This formula is the basis of the widely used Houbolt integrator (9)

and E_y is given in (12b). The temporal stability of (36) may be examined by seeking a nontrivial solution of the form

$$\underline{z}_n = \lambda \, \underline{z}_{n-1} \tag{38}$$

where

$$\underline{z} = (\dot{\underline{x}}, \underline{x}, \underline{y}, \dot{\underline{y}})^T$$

and requiring a bounded solution for (36), viz,

$$| \lambda | \leq 1 \tag{39}$$

Difference equations similar to (36) may also be obtained for the DE formulation. Evaluation of the stability condition (39) for various time-integrator/predictor combinations leads to tedious algebraic manipulations (Appendix C). Table 5 summarizes the results for the single-pass implementation of the formulations listed in Table 2.

TABLE 5. Stability Characteristics of Single-Pass Solutions

Formulation	Stability Properties
Pressure Extrapolation (PE)	$\chi < 4$ for trapezoidal rule[a]
Pressure Integral Extrapolation (PIE)	Unconditionally stable[b] for predictor cases I, II[c]
Displacement Extrapolation (DE)	Unconditionally stable[b] for predictor cases I, III[c] when trapezoidal rule is used[d]

[a] See Figure 1.

[b] "Unconditionally stable" means temporal stability for any feasible combination of physical parameters and integration stepsize.

[c] See Table 4.

[d] Allowable predictors depend on integration method used.

6.3 OBSERVATIONS ON SINGLE-PASS SOLUTION STABILITY

The single-pass stability properties listed in Table 5 account for the combined effects of the predictor and the time-integrator. The results indicate that the two augmented formulations are capable of delivering stable single-pass solutions provided that the extrapolation accuracy is suitably restricted. Such restrictions are, in general, affected by the integration method. For example, application of the trapezoidal rule to the DE formulation limits the extrapolator accuracy to first order (case IV of Table 4), whereas the application of an A-stable backward-difference scheme allows the use of all of the predictors listed in Table 4.

We recall that the two stabilized formulations can, if iterated to convergence, attain the unconditional stability of the fully-implicit solution procedure (cf. Table 3 and Figure 2), regardless of the choice of extrapolator. This observation raises again the issue of finding a cost-minimization compromise between a single-pass solution process with small time increments and an iterated solution process with larger time increments. A resolution of this issue must await the accumulation of experience in the application of these new techniques to actual linear and nonlinear fluid-structure interaction problems.

Finally, it should be mentioned that stability analyses of the differential-difference equations pertaining to the single-pass PIE and DE formulations were also performed using integral-transform techniques similar to those used for the PE formulation. These analyses provided valuable insight into the sensitivity of the stability characteristics to the various parameters appearing in the model formulations. The results will not be reported here, however, because of the length and complexity of the algebraic manipulations involved.

SECTION VII

NUMERICAL EXPERIMENTS

A series of numerical experiments was conducted with dual objectives: to verify the predictions of the convergence and stability analyses, and to assess the global accuracy of the staggered solution procedures. We have adopted a direct accuracy assessment over an analytical accuracy analysis, as the former provides an overall (global) measure of accuracy, which results from the combined effects of integration algorithm and implementation form [10], as well as extrapolation process. The accuracy measure chosen for the present study is

$$\varepsilon = \left[\sum_{i=1}^{N} (z_i^E - z_i^C)^2 \Big/ \sum_{i=1}^{N} (z_i^E)^2 \right]^{1/2} \tag{40}$$

where the superscripts $(\,)^E$ and $(\,)^C$ denote the exact and computed solutions at the discrete time station $t = t_i$, respectively, and N is the total number of time steps taken to evaluate ε. The exact solutions were obtained by using the characteristic roots of the fully-implicit procedure (21) and applying the initial conditions

$$\begin{aligned} x(0) &= (\xi\ \chi/\Omega)^2 \\ \dot{x}(0) &= 1 \\ \dot{y}(0) &= \xi \end{aligned}$$

These values produce reasonably scaled response histories for all three response variables of interest.

A number of implicit, one-derivative, A-stable LMS methods were used for the numerical solution of each of the (4), among them being the trapezoidal rule and the backward-difference operators of Park [11] and Gear [12]. In the results to be presented here, the trapezoidal rule was used to advance the structural response while the Park three-step method was applied to the solution of the fluid equation.

Error comparisons after 20 steps were made for the structural displacement $x(t)$ and velocity $\dot{x}(t)$ as well as the fluid pressure $\dot{y}(t)$; however, only the displacement results will be shown. Accuracy assessments were carried out for the parameter range

$$1 \le \chi \le 10, \quad 0.01 \le \Omega \le 1.0, \quad 0.0001 \le \Psi \le 0.1,$$

with the results being relatively insensitive to Ψ . For this reason, comparisons are shown here only for $\Psi = 0.1$, which value usually produced the greatest error.

Figure 6 shows a comparison between the pressure integral extrapolation scheme, denoted by x^{PIE}, versus the displacement extrapolation scheme, denoted by x^{DE}. In each case a two-step standard linear extrapolation method (case III of Table 4) was used. Although the PIE solution displays superior accuracy, this scheme violates the practical requirement (justified in the following section) that the structural equations be left unchanged. It is therefore important to show that the accuracy of the DE scheme can be improved without incurring a substantial increase in computation time. Two immediate ways of accomplishing this objective are: the use of a three-step extrapolation method (case IV of Table 4), and the performance of one iteration on the fluid equation solution. The latter effectively amounts to an additional half-pass through the solution strategy.

As the integration of the structural equations normally controls the computation time in large-scale problems, this additional iteration can be carried out with a modest increase in the total run cost.

The resulting improvement in the accuracy of the DE procedure is shown in Figures 7 and 8, where the first subscript indicates whether a two-step or a three-step extrapolation method is used and the second subscript denotes the number of iterations made on the fluid equation. Hence $x^{DE}_{2,0}$ is identical to x^{DE} in Figure 6. As can be seen, the solution accuracy is more sensitive to the extrapolation scheme used; however, the value of applying one iteration to the fluid equation is also apparent. Similar accuracy improvements were observed for the velocity and pressure components of the solution.

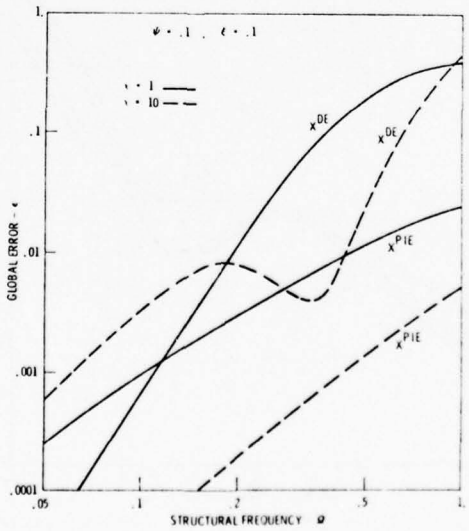

Figure 6 Global Error for PIE and DE Forms

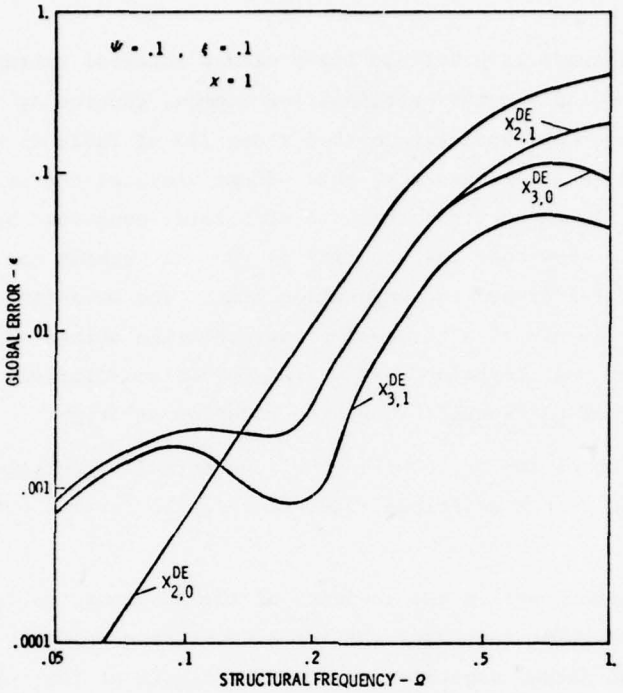

Figure 7 Global Error for Improved DE Forms, $\chi = 1$

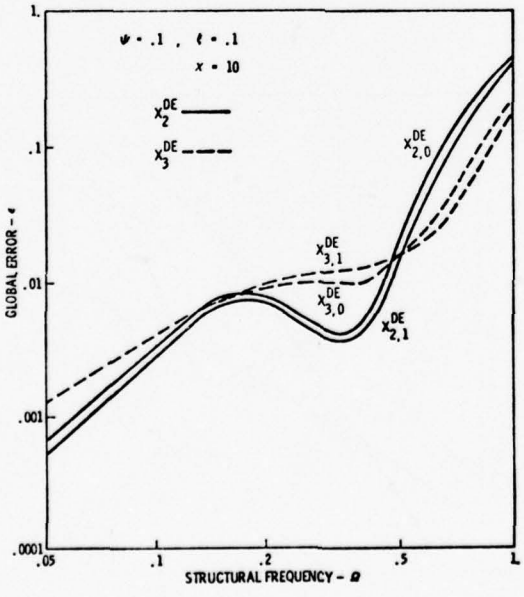

Figure 8 Global Error for Improved DE Forms, $\chi = 10$

SECTION VIII

IMPLEMENTATION CONSIDERATIONS

Thus far we have concentrated on stabilization of the staggered solution procedure; we have succeeded in developing several stabilized forms of the two degree-of-freedom system (4). Application of the two formulations of greatest interest to the original matrix system (1) provides the equations shown in Table 6. Before selecting one of these formulations for implementation in a fluid-structure analysis code, it is necessary that we discuss the practical implications associated with such a decision.

If there were no a priori constraints with regard to software development, i.e., the program developer had complete freedom to construct both the structural and fluid analyzers from scratch, the overriding selection factor would probably be the accuracy characteristics displayed by each formulation. As it is, there now exist many large-scale linear and nonlinear structural analyzers that incorporate capabilities for transient response analysis.

TABLE 6. Matrix Implementation Forms for Stabilized Procedures

Formulation	Implementation
Pressure Integral Extrapolation (PIE)	$\underset{\sim}{M}\,\ddot{\underline{u}} + (\underset{\sim}{D} + \rho\, c\, \underset{\sim}{T}\,\underset{\sim}{A}\,\underset{\sim}{T}^{T})\,\dot{\underline{u}} + \underset{\sim}{K}\,\underline{u} = \underline{f}_s + \underline{r} - \underset{\sim}{T}\,\underset{\sim}{A}\,(\underline{p}^I - \rho\, c\, \dot{\underline{u}}^I) + \rho\, c\, \underset{\sim}{T}\,\underset{\sim}{A}\,\underset{\sim}{M}_f^{-1}\,\underset{\sim}{A}\,\underline{q}$ $\underset{\sim}{A}\,\dot{\underline{q}} + \rho\, c\, \underset{\sim}{A}\,\underset{\sim}{M}_f^{-1}\,\underset{\sim}{A}\,\underline{q} = \rho\, c\, \underset{\sim}{A}\,(\underset{\sim}{T}^T\,\dot{\underline{u}} - \dot{\underline{u}}^I)$
Displacement Extrapolation (DE)	$\underset{\sim}{M}\,\ddot{\underline{u}} + \underset{\sim}{D}\,\dot{\underline{u}} + \underset{\sim}{K}\,\underline{u} = \underline{f}_s + \underline{r} - \underset{\sim}{T}\,\underset{\sim}{A}\,(\dot{\underline{q}} + \underline{p}^I)$ $\underset{\sim}{A}\,\ddot{\underline{q}} + \rho\, c\, (\underset{\sim}{A}\,\underset{\sim}{M}_f^{-1}\,\underset{\sim}{A} + \underset{\sim}{A}\,\underset{\sim}{M}^{-G}\,\underset{\sim}{A})\,\dot{\underline{q}} = -\rho\, c\, \underset{\sim}{A}\,\ddot{\underline{u}}^I - \rho\, c\, \underset{\sim}{A}\,\underset{\sim}{M}^{-G}\,\underset{\sim}{A}\,\underline{p}^I + \rho\, c\, \underset{\sim}{A}\,\underset{\sim}{M}^{-G}\,\underset{\sim}{C}^{-1}\,\underset{\sim}{T}^T\,(\underline{f}_s + \underline{r} - \underset{\sim}{D}\,\dot{\underline{u}} - \underset{\sim}{K}\,\underline{u})$ where $\underset{\sim}{M}^{-G} = \underset{\sim}{C}^T\,(\underset{\sim}{T}^T\,\underset{\sim}{M}\,\underset{\sim}{T})^{-1}\,\underset{\sim}{C}$, $\underset{\sim}{C} = \underset{\sim}{T}^T\,\underset{\sim}{T}$

Inspection of Table 6 reveals that only the DE formulation has no impact upon the structural equations of motion, while the PIE formulation (as well as the other, more complicated, formulations) requires the addition of a damping term, $\rho\, c\, \underset{\sim}{T}\,\underset{\sim}{A}\,\underset{\sim}{T}^T$, to the left-hand side of the structural equation. This term can be expected to have an adverse effect

upon the sparseness characteristics of the dynamic coefficient matrix [the multi-degree-of-freedom analog of E_x in Eqs. (11) and (36)], because each fluid boundary element on the contact or "wet" surface B will normally overlap several structural elements[†]. Additional nonzero coefficients then appear outside the "profile" of the structural stiffness matrix in entry positions pertaining to the wet structural displacements on B. As matrix connectivity characteristics are generally controlled by the structural grid information, extensive and expensive software modifications would be required to include such a damping tern in existing "dry-structure" analyzers.

For the analysis of linear structures, a general-purpose, stand-alone integration package based on available A-stable LMS methods could be built for the PIE and other formulations, which would accept, as input data, preprocessed matrices assembled by existing linear structural analysis codes (with, perhaps, some restrictions on sparse-matrix storage formats). However, for structures exhibiting nonlinear behavior, such an undertaking would necessitate the coupling of the nonlinear solver with the dedicated integration package to provide continuously updated information in the form of factored matrices, pseudo-force vectors, and the like. In this case, the driving consideration would certainly be preservation of the autonomy of the structural analyzer, a restriction that precludes the use of either the PIE or other forms.

An additional argument that reinforces this conclusion is the fact that the DAA is only the lowest-order member of a family of surface interaction approximations [3]. The next member of that family is characterized by a second-order matrix ODE that would replace (1b). The inclusion of a higher derivative of the scattered pressure has the effect of adding widely-connected matrix terms to both the damping and stiffness matrices in the structural equations if the equivalents of the PIE and other formulations are adopted.

In summary, it seems clear that the displacement extrapolation formulation is the only stabilized procedure that satisfies the practical requirements of modularity and avoids the proliferation of special-purpose versions of existing structural analyzers.

[†]The fluid discretization can be much coarser than the structural discretization because the calculation of spatial displacement gradients is only required for the structural model in order to obtain strains and stresses.

SECTION IX

CONCLUDING REMARKS

The original goal of this investigation was to find an optimal implementation of the staggered solution strategy for the structure/DAA equations, with the model equations (3) or (4) as a point of departure. It was hoped that such an implementation would display adequate stability and accuracy properties to provide a suitable alternative to the fully-implicit (simultaneous-solution) approach, but without the computational drawbacks of the latter. Although that goal was attained beyond our expectations, the study guidelines had to be frequently redefined along the way.

It is a common attribute of intricate research projects that essential ingredients of the problem, i.e., those aspects crucial to success or failure, are seldom recognized in advance. The work reported here is no exception. An extensive initial series of parametric studies aimed at extending the stability limit of the conventional staggered solution procedure failed to yield satisfactory results. When attempts to introduce artificial damping terms proved fruitless, and when we were seriously considering the adoption of explicit integration methods, the augmentation concept was tried, which led to the derivation of the PIE formulation. That serendipitous discovery prompted a systematic development of other formulations and the final selection of the displacement extrapolation formulation.

The interpretation of staggered solution procedures from the viewpoint of control theory emerged in final form as this report was being prepared. This interpretation is deemed important for a variety of reasons:

- The effects of the predictor can be incorporated into differential-difference equations, thus isolating the effects of the integration method. (The latter can in fact be included, if desired, by adjoining to the characteristic determinant terms resulting from a Laplace-transformation of the integration operator [13].)
- A large body of control theory techniques, such as frequency bandwidth reduction, damping augmentation, etc., can be applied to the stabilization of the system in transform space, and such remedies reverted to the time domain and interpreted in terms of computational procedures; see, for example, [14, 15].
- A block representation, such as the one shown in Figure 5, provides a convenient framework for setting up parameter studies using a digital or analog computer.
- The interpretation is applicable to general classes of coupled field problems, rather than being confined to fluid-structure interaction analysis.

With regard to the last of these, there is presently a growing interest in the application of computerized analysis methods to a host of problems that are modeled through coupled-field evolutionary equations arising in geomechanics, biomechanics, thermoelasticity and magnetohydrodynamics, to cite only a few. Staggered solution procedures appear particularly attractive when software modules (analyzers) are available for processing the individual uncoupled problems. These modules can be connected to form a serially-executable "analyzer network" through interfacing mechanisms based on the prediction of appropriate subsets of the complete solution vector. Stabilization of these mechanisms at the governing ODE level is most effective for avoiding "delayed feedback" instability. Once satisfactory stabilized formulations are synthesized, accuracy and implementation considerations can be used to select the most desirable formulation and associated extrapolation formulas.

REFERENCES

1. Geers, T. L., "Transient Response Analysis of Submerged Structures", in Finite Element Analysis of Transient Nonlinear Behavior, Belytschko, T., Osias, J. R. and Marcal, P. V., eds, AMD-Vol. 14, ASME, New York, N. Y., 1975, pp 59-84.

2. Geers, T. L., "Residual Potential and Approximate Methods for Three-Dimensional Fluid-Structure Interaction Problems", J. Acoust. Soc. Am., Vol. 49, No. 5, May 1971, pp 1505-1510.

3. Geers, T. L. and Felippa, C. A., "Doubly Asymptotic Approximations for Transient Motion of Submerged Structures", Proc. of the 6th Canadian Congress of Applied Mechanics, Vancouver, Canada, May 29-June 3, 1977, pp 693-694; full paper to be submitted to J. Acoust. Soc. Am.

4. Lapidus, L. and Seinfeld, J. H., Numerical Solution of Ordinary Differential Equations, Academic Press, New York, N. Y., 1971.

5. Bellman, R. and Cooke, K. L., Differential-Difference Equations, Academic Press, New York, 1963.

6. Takahashi, T., Mathematics of Automatic Control, Holt, Rinehart and Winston, New York, N. Y., 1966.

7. Nyquist, H., "Regeneration Theory", Bell System Tech. J., Vol. II, 1932, pp 126-147.

8. Gibson, J. E., Nonlinear Automatic Control, McGraw-Hill, 1963.

9. Houbolt, J. C., "A Recurrence Matrix Solution for the Dynamic Response of Elastic Aircraft", J. Aero. Sci., Vol. 17, 1950, pp 540-550.

10. Felippa, C. A. and Park, K. C., "Computational Aspects of Time Integration Procedures in Structural Dynamics", LMSC-D556247, Lockheed Palo Alto Research Laboratory, Palo Alto, CA, January 1977; to appear in J. Appl. Mech.

11. Park, K. C., "An Improved Stiffly Stable Method for Direct Integration of Nonlinear Structural Dynamic Equations", J. Appl. Mech., Vol. 42, No. 2, 1975, pp 464-470.

12. Gear, C. W., "Numerical Integration of Stiff Ordinary Differential Equations", Report No. 221, Department of Computer Science, University of Illinois, 1967.

13. Brayton, R. K. and Willoughby, R. A., "On the Numerical Integration of a Symmetric System of Differential-Difference Equations of Neutral Type", J. Math. Anal. Appl., Vol. 18, 1967, pp 182-189.

14. Fowler, M. E., "A New Numerical Method for Simulation", Simulation, Vol. 4, May 1965, pp 324-330.

15. Smith, J. M., "Recent Developments in Numerical Integration", J. Dynamic Systems, Measurement, and Control, Trans. ASME, March 1974, pp 61-70.

16. DeRuntz, J. A. and Geers, T. L., "Added Mass Computation by the Boundary Integral Method", to appear in Int. J. Numer. Meth. Engrg., 1977.

17. Geers, T. L., unpublished study, April 1977.

18. Junger, M. C. and Feit, D., Sound, Structures, and Their Interaction, the MIT Press, Cambridge, Mass., 1972.

APPENDIX A

DERIVATION OF MODEL EQUATIONS

Consider the following form of the homogeneous system (2)

$$\begin{aligned} \underset{\sim}{M}\,\ddot{\underline{u}} + \underset{\sim}{K}\,\underline{u} &= -\underset{\sim}{T}\,\underset{\sim}{A}\,\dot{\underline{q}} \\ \underset{\sim}{A}\,\dot{\underline{q}} + \rho\, c\, \underset{\sim}{B}\,\underline{q} &= \rho\, c\, \underset{\sim}{A}\,\underset{\sim}{T}^{T}\,\dot{\underline{u}} \end{aligned} \tag{A-1}$$

in which $\underset{\sim}{B} = \underset{\sim}{A}\,\underset{\sim}{M}_f^{-1}\,\underset{\sim}{A}$. Equations (A-1) are obtained upon setting $\underset{\sim}{D} = \underset{\sim}{0}$ (no structural damping) and premultiplying the fluid equation by $\underset{\sim}{A}^{T}\,\underset{\sim}{M}_f^{-1} = \underset{\sim}{A}\,\underset{\sim}{M}_f^{-1}$; the latter operation makes the coupling matrices in the right-hand side of (A-1) the transpose of one another. The symmetric algebraic eigenproblems associated with the left-hand side of (A-1) are

$$\begin{aligned} (-\bar{\omega}_i^{2}\,\underset{\sim}{M} + \underset{\sim}{K})\,\underline{u}_i &= \underline{0}, \qquad i = 1, \ldots n_s \\ (\lambda_j\,\underset{\sim}{A} + \underset{\sim}{B})\,\underline{q}_j &= \underline{0}, \qquad j = 1, \ldots n_f \end{aligned} \tag{A-2}$$

The $\underline{u}_i$ are the dry structural modes (also called in vacuo modes) pertaining to the undamped natural frequencies $\bar{\omega}_i$. The $\underline{q}_j$ are fluid boundary modes associated with the pressure-decay exponents $\lambda_j = \rho\,\ell\,\mu_j$. (These fluid modes are discrete analogs of the eigenfunctions of the added mass tensor associated with the Laplace equation, subject to appropriate orthonormality conditions with respect to surface area [16].) In accordance with (A-2), we introduce the transformations

$$\underline{u} = \underset{\sim}{S}\,\underline{w}\,; \qquad \underline{q} = \underset{\sim}{F}\,\underline{g} \tag{A-3}$$

where the matrices $\underset{\sim}{S}$ and $\underset{\sim}{F}$ are formed with the dry-structure and fluid-boundary modes, respectively, lined up as columns of unit length, and the vectors $\underline{w}$ and $\underline{g}$ collect the associated mode amplitudes (generalized coordinates). The transformed system (A-1) is then

$$\begin{aligned} \underset{\sim}{m}_s\,\ddot{\underline{w}} + \underset{\sim}{k}_s\,\underline{w} &= -\underset{\sim}{S}^{T}\,\underset{\sim}{T}\,\underset{\sim}{A}\,\underset{\sim}{F}\,\dot{\underline{g}} = -\underset{\sim}{H}\,\underline{g} \\ \underset{\sim}{a}\,\dot{\underline{g}} + \rho c \underset{\sim}{b}\underline{g} &= \rho\, c\, \underset{\sim}{F}^{T}\,\underset{\sim}{A}\,\underset{\sim}{T}^{T}\,\underset{\sim}{S}\,\dot{\underline{w}} = \rho\, c\, \underset{\sim}{H}^{T}\,\dot{\underline{w}} \end{aligned} \tag{A-4}$$

where $\underset{\sim}{m}_s$, $\underset{\sim}{k}_s$, $\underset{\sim}{a}$ and $\underset{\sim}{b}$ are diagonal matrices of generalized quantities:

$$\underset{\sim}{m}_s = \underset{\sim}{S}^T \underset{\sim}{M} \underset{\sim}{S}, \qquad \underset{\sim}{k}_s = \underset{\sim}{S}^T \underset{\sim}{K} \underset{\sim}{S}$$

$$\underset{\sim}{a} = \underset{\sim}{F}^T \underset{\sim}{A} \underset{\sim}{F} \tag{A-5}$$

$$\underset{\sim}{b} = \underset{\sim}{F}^T \underset{\sim}{B} \underset{\sim}{F} = \underset{\sim}{a} (\underset{\sim}{F}^T \underset{\sim}{M}_f \underset{\sim}{F})^{-1} \underset{\sim}{a} = \underset{\sim}{a} \underset{\sim}{m}_f^{-1} \underset{\sim}{a}$$

Although the left side of (A-4) is uncoupled, each dry structural mode will, in general, be coupled to each fluid boundary mode through the right-hand side terms. Consequently, for each mode pair $\underline{u}_i$, $\underline{q}_j$, we obtain a two degree-of-freedom system in the associated generalized coordinates w_i and g_j :

$$\begin{aligned} m_{si} \ddot{w}_i + k_{si} w_i &= -\varphi_{ij} a_j \ddot{g}_j \\ a_j g_j + \rho c b_j g_j &= \rho c a_j \varphi_{ji} \ddot{w}_i \end{aligned} \tag{A-6}$$

In (A-6), the φ_{ij} are modal coupling coefficients between the i-th structural mode and the j-th fluid boundary mode, i.e.,

$$\varphi_{ij} = \frac{h_{ij}}{a_j} = \frac{\underline{u}_i^T \underset{\sim}{T} \underset{\sim}{A} \underline{q}_j}{\underline{q}_j^T \underset{\sim}{A} \underline{q}_j} = \frac{\underline{r}_i^T \underset{\sim}{A} \underline{q}_j}{\underline{q}_j^T \underset{\sim}{A} \underline{q}_j} \tag{A-7}$$

where

$$\underline{r}_i = \underline{u}_i^T \underset{\sim}{T} . \tag{A-8}$$

We will now show that $| \varphi_{ij} | \leq 1$ if all entries of the structure-to-fluid grid transformation matrix are nonnegative (a restriction that can always be met by using appropriate "area-lumping" schemes). Equilibrium of forces normal to the contact surface demands that the sum of entries, $t_{k\ell}$ of each column $\underline{t}_\ell$ of $\underset{\sim}{T}$ be unity:

$$\sum_{k=1}^{n_s} t_{k\ell} = \sum_k | t_{k\ell} | = 1 \tag{A-9}$$

Hence

$$\| \underline{t}_\ell \|_2^2 = \underline{t}_\ell^T \underline{t}_\ell \leq \left(\sum_k | t_{k1} | \right)^2 = 1 \tag{A-10}$$

Using the norm inequality $\| \underline{x}^T \underline{y} \| \leq \| \underline{x} \| \cdot \| \underline{y} \|$, we can easily show that $\| \underline{r}_i \|_2 \leq 1$.

Now from (A-7) we obtain

$$(\underline{q}_j \, \varphi_{ij} - \underline{r}_i)^T \, \underset{\sim}{A} \, \underline{q}_j = 0 \tag{A-11}$$

As $\underset{\sim}{A}$ is positive definite and $\underline{q}_j$ is not identically zero, it follows that the vector in parenthesis must be orthogonal to $\underset{\sim}{A} \, \underline{q}_j$. Premultiplying that vector by $\underline{q}_j^T$ and solving for φ_{ij}, we obtain the desired result

$$\varphi_{ij} = \frac{\underline{q}_j^T \, \underline{r}_i}{\underline{q}_j^T \, \underline{q}_j} = \underline{q}_j^T \, \underline{r}_i \leq 1 \tag{A-12}$$

Eq. (A-12) indicates that setting $\varphi_{ij} = 1$ in (A-6) implies a conservative assumption on the modal coupling, which is the essential source of stability difficulties in the staggered solution procedures. The worst modal coupling case, i.e., $\varphi_{ij} = 1$, occurs when both structural and fluid boundary modes coincide, as in the case of breathing motions of a submerged spherical shell. Assuming identical surface grids for this case, we have $\underline{u}_i = \underline{q}_j \, \underset{\sim}{T} = \underset{\sim}{I}$ and $\varphi_{ij} = 1$.

APPENDIX B

SUBMERGED SPHERICAL SHELL

To get an idea of the range of values assumed by the various parameters that appear in the study of the staggered solution procedures, it is instructive to study a closed, thin spherical shell submerged in an infinite fluid. The dry-structure and fluid-boundary modes for the continuum problem coalesce and can be analytically expressed in terms of Legendre polynomials in $\cos\theta$, θ being the meridional angle. An analysis of the modal spectrum [17] pertaining to axisymmetric modal motions with n circumferential waves gives for the generalized structural mass, stiffness, fluid mass and contact areas,

$$\begin{aligned} m_{sn} &= 4\pi\rho_s\, tr^2\, [1 + n\,(n+1)\zeta_n^2]\,/(2n+1) \\ k_{sn} &= m_{sn}\,\bar{\omega}_{sn}^2 \\ m_{fn} &= 4\pi\rho\, r^3\,/[(n+1)\,(2n+1)] \\ a_n &= 4\pi\, r^2\,/\,(2n+1) \end{aligned} \tag{B-1}$$

where ρ_s, t and r are the shell density, thickness and radius, respectively, $\bar{\omega}_{sn}$ denotes modal natural frequency [not to be confused with the reduced frequency ω defined in (5b)] and ζ_n are ratios of tangential to radial modal amplitudes, given by [18, Ch. 10]

$$\zeta_n = (1+\nu)\,/\,[-\hat{\omega}_n^2 + n^2 + n + (1-\nu)] \tag{B-2}$$

where ν is Poisson's ratio, and the $\hat{\omega}_n$ are dimensionless in-vacuo natural frequencies ($\bar{\omega}_n$ normalized to c_s/r, c_s being the plate velocity for the shell material). The dimensionless parameters ξ, ω and μ can be obtained from Eqs. (5), in which $\ell = r$, as

$$\begin{aligned} \xi_n &= [1 + n\,(n+1)\,\zeta_n^2]\,\rho_s t/\rho r) \\ \omega_n &= \xi^{\frac{1}{2}}\hat{\omega}_n\, c_s/c \\ \mu_n &= n+1 \end{aligned}$$

Values of ξ, ω and μ are compiled in Table 7 for a steel shell in water ($c_s/c \cong 3.53$, $\rho_s/\rho \cong 7.67$, $\nu = 0.30$) with a thickness-to-radius ratio of 0.01. The lower (upper) eigenfrequency branch embodies predominantly flexural (membrane) motions.

Note that the lowest values of these parameters are determined by physical and geometric characteristics of the fluid-structure problem, whereas the high values are determined by truncation of the modal spectrum. For the discrete model, the largest values are essentially functions of the mesh fineness. These considerations should be helpful in the order-of-magnitude assessment of the parameter value range for more complex problems.

TABLE 7. Values of ξ, ω, and μ for Some Axisymmetric Modes of a Steel Shell in Water with t/r = 0.01

Mode Order Branch n	ζ_n	$\hat{\omega}_n$	ξ_n	ω_n	μ_n
Lower 1	1.000	0	0.230	0	2
2	0.270	0.701	0.110	0.821	3
3	0.123	0.830	0.091	0.882	4
n>>1	$\sim n^{-2}$	$\sim 1-1/2n$	~ 0.077	~ 0.977	n + 1
Upper 0	0	1.61	0.077	0.977	1
1	-0.500	1.98	0.115	2.37	2
2	-0.616	2.72	0.251	4.81	3
3	-0.680	3.64	0.502	9.10	4
n>>1	$\sim -n/n+1$	$\sim (n^2 + 3)^{\frac{1}{2}}$	$\sim 0.077n^2$	$\sim 0.98n^2$	n + 1

APPENDIX C

A STABILITY ANALYSIS OF THE PIE FORMULATION

Let us write (6) and (7) as

$$\rho\ (\underline{Z}_{n}-k) - \delta\sigma(\dot{\underline{Z}}_{n-k}) \;=\; 0,\ k = 1\ ,\ -\ -\ ,\ m\ . \tag{C-1}$$

where

$$\rho\ (\underline{Z}_{n-k}) = \sum_{k=0}^{m} \alpha_k\ \underline{Z}_{n-k}\ ,\ \sigma\ (\dot{Z}_{n-k}) \;=\; \sum_{k=0}^{m} \beta_k\ \dot{\underline{Z}}_{n-k} \tag{C-2}$$

and the PIE model equations in Table 2 as

$$\begin{bmatrix} 0 & 1 & 0 \\ \xi & 0 & 0 \\ 0 & 0 & 1 \end{bmatrix} \dot{Z}_n + \begin{bmatrix} -1 & 0 & 0 \\ 1 & \omega^2 & -\mu \\ 0 & 0 & \mu \end{bmatrix} Z_n = \begin{bmatrix} 0 \\ 0 \\ \dot{x}_n^P \end{bmatrix} \tag{C-3}$$

where $\underline{Z} = [\dot{x},\ x,\ y]^T$

For illustrative purposes, introduce the first-order extrapolator [see (35) and Table 4].

$$\dot{\underline{x}}_n^P \;=\; 2\dot{\underline{x}}_{n-1} - \dot{\underline{x}}_{n-2} \tag{C-4}$$

combining (C-1) through (C-3), we obtain

$$\begin{bmatrix} 0 & 1 & 0 \\ \xi & 0 & 0 \\ 0 & 0 & 1 \end{bmatrix} \rho(Z_{n-k}) + \delta \begin{bmatrix} -1 & 0 & 0 \\ 1 & \omega^2 & -\mu \\ 0 & 0 & \mu \end{bmatrix} \sigma(Z_{n-k}) = \delta \begin{bmatrix} 0 \\ 0 \\ \sigma(\dot{X}_{n-k}^P) \end{bmatrix} \tag{C-5}$$

Substitution of (38) into this equation then yields

$$\left\{ \begin{bmatrix} 0 & 1 & 0 \\ \xi & & 0 \\ 0 & 0 & 1 \end{bmatrix} \rho(\lambda) + \delta \begin{bmatrix} -1 & 0 & 0 \\ 0 & \omega^2 & -\mu \\ -\frac{2}{\lambda} - \frac{1}{\lambda^2}, & 0 & \mu \end{bmatrix} \sigma(\lambda) \right\} \underline{Z}_{n-m} = 0 \tag{C-6}$$

where

$$\rho(\lambda) = \sum_{k=0}^{m} \alpha_k \lambda^{m-k} \quad , \quad \sigma(\lambda) = \sum_{k=0}^{m} \beta_k \lambda^{m-k} \tag{C-7}$$

Now a nontrivial solution of (C-6) exists only when

$$\det \left\{ \begin{bmatrix} 0 & 1 & 0 \\ \xi & 0 & 0 \\ 0 & 0 & 1 \end{bmatrix} \rho(\lambda) + \delta \begin{bmatrix} -1 & 0 & 0 \\ 1 & \omega^2 & -\mu \\ -\frac{2}{\lambda} - \frac{1}{\lambda^2} & 0 & \mu \end{bmatrix} \sigma(\lambda) \right\} = 0 \tag{C-8}$$

from which we obtain the following characteristic equation

$$\rho^3(\lambda) + \delta \mu \rho(\lambda) \sigma(\lambda) \left[\rho(\lambda) - \frac{\delta\sigma}{\xi}(\lambda)(2\lambda - 1)/\lambda^2 \right]$$

$$\frac{\delta^3\omega^2\mu}{\xi} \sigma^3(\lambda) + \frac{\delta^2\omega^2}{\xi}\sigma^2(\lambda) \rho(\lambda) + \frac{\delta}{\xi} \rho^2(\lambda) \sigma(\lambda) + \frac{\delta^2\mu}{\xi} \rho(\lambda) \sigma^2(\lambda) = 0 \tag{C-9}$$

Therefore, the search for unconditional stability is reduced to determining the complete absence of any root of (C-9) with magnitude greater than unity for all possible values of ωh , μh , and h/ξ in combination with the time integrator and extrapolator used. The results of such determinations are summarized in Table 5.

DISTRIBUTION LIST

DEPARTMENT OF DEFENSE

Assistant to the Secretary of Defense
Atomic Energy
ATTN: ATSD (AE)

Director
Defense Advanced Rsch. Proj. Agency
ATTN: A. Tachmindji
ATTN: K. Kresa
ATTN: MISD/PM
ATTN: R. Chapman

Director
Defense Civil Preparedness Agency
Assistant Director for Research
ATTN: Admin. Officer

Defense Documentation Center
Cameron Station
12 cy ATTN: TC

Director
Defense Intelligence Agency
ATTN: DI-7E
ATTN: RDS-3A
ATTN: DB-4C, E. O'Farrell
ATTN: DT-1C
ATTN: DT-2, Wpns. & Sys. Div.

Director
Defense Nuclear Agency
ATTN: DDST
ATTN: TISI
2 cy ATTN: SPSS
3 cy ATTN: TITL

Chairman
Dept. of Defense Explo. Safety Board
ATTN: DD/S&SS

Commander
Field Command, DNA
ATTN: FCPR
ATTN: FCPR, Colonel J. Hill

Director
Interservice Nuclear Weapons School
ATTN: Document Control

Director
Joint Strat. Tgt. Planning Staff
ATTN: STINFO Library

Chief
Livermore Division, Fld. Command, DNA
Lawrence Livermore Laboratory
ATTN: FCPRL

Commandant
NATO School (SHAPE)
ATTN: U.S. Documents Officer

Under Secretary of Def. for Rsch. & Engrg.
ATTN: S&SS (OS)

DEPARTMENT OF THE ARMY

Dep. Chief of Staff for Rsch. Dev. & Acq.
ATTN: DAMA-AOA-M
ATTN: DAMA-CSM-N, LTC G. Ogden

Deputy Chief of Staff for Ops. & Plans
ATTN: MOCA-ADL

Commander, Harry Diamond Laboratories
ATTN: DELHD-TI
ATTN: DELHD-NP

Commander
Redstone Scientific Information Ctr.
U.S. Army Missile Command
ATTN: Chief, Documents

Commander
U.S. Army Armament Command
ATTN: Tech. Lib.

Director
U.S. Army Ballistic Research Labs.
ATTN: Tech. Lib., E. Baicy

Commander
U.S. Army Communications Cmd.
ATTN: Tech. Lib.

Director
U.S. Army Engr. Waterways Exper. Sta.
ATTN: W. Flathau
ATTN: J. Strange
ATTN: Tech. Lib.

Commander
U.S. Army Mat. & Mechanics Rsch. Ctr.
ATTN: R. Shea
ATTN: Tech. Lib.

Commander
U.S. Army Materiel Dev. & Readiness Cmd.
ATTN: DRXAM-TL

Commander
U.S. Army Mobility Equip. R&D Ctr.
ATTN: DRDME-WC

Commander
U.S. Army Nuclear & Chemical Agency
ATTN: Library

Commandant
U.S. Army War College
ATTN: Library

DEPARTMENT OF THE NAVY

Chief of Naval Material
ATTN: MAT 0323

Chief of Naval Operations
ATTN: OP 981
ATTN: OP 03EG

DEPARTMENT OF THE NAVY (Continued)

Chief of Naval Research
ATTN: Code 715
2 cy ATTN: Code 474, N. Perrone

Officer-in-Charge
Civil Engineering Laboratory
Naval Construction Battalion Center
ATTN: R. Odello
ATTN: Technical Library

Commander
David W. Taylor Naval Ship R&D Ctr.
ATTN: Code 177
ATTN: Code 2740, Y. Wang
ATTN: Code L42-3, Library
ATTN: Code 174
ATTN: Code 17
ATTN: Code 1740.1
ATTN: Code 1740.5
ATTN: Code 1740.6
ATTN: Code 1962
ATTN: Code 19
ATTN: Code 1903
ATTN: Code 11
2 cy ATTN: Code 172

Commander
Naval Electronic Systems Command
Naval Electronic Systems Cmd. Hqs.
ATTN: PME 117-21A

Commander
Naval Facilities Engineering Command
Headquarters
ATTN: Code 09M22C

Commander
Naval Ocean Systems Center
ATTN: Technical Library

Superintendent (Code 1424)
Naval Postgraduate School
ATTN: Code 2124, Tech. Rpts. Librarian

Director
Naval Research Laboratory
ATTN: Code 840, J. Gregory
ATTN: Code 2600, Tech. Lib.
3 cy ATTN: Code 8403A, G. O'Hara

Commander
Naval Sea Systems Command
ATTN: Code 03511, C. Pohler
ATTN: ORD-91313, Lib.

Commander
Naval Ship Engineering Center
ATTN: NSEC 6110.01
ATTN: Technical Library
ATTN: NSEC 6105
ATTN: NSEC 6120D
ATTN: NSEC 6105G
ATTN: 6105C1

Officer-in-Charge
Naval Surface Weapons Center
3 cy ATTN: Code WA501, Navy Nuc. Prgms. Off.

DEPARTMENT OF THE NAVY (Continued)

Commander
Naval Surface Weapons Center
Dahlgren Laboratory
ATTN: Technical Library

Commanding Officer
Naval Underwater Systems Center
ATTN: Code EM, J. Kalinowski

Commander
Naval Weapons Center
ATTN: Code 533, Tech. Lib.

Commanding Officer
Naval Weapons Evaluation Facility
ATTN: Technical Library

Director
Strategic Systems Project Office
ATTN: NSP-272
ATTN: NSP-43, Tech. Lib.

DEPARTMENT OF THE AIR FORCE

AF Geophysics Laboratory, AFSC
ATTN: SUOL, Rsch. Lib.

AF Institute of Technology, AU
ATTN: Library, AFIT Bldg. 640, Area B

AF Weapons Laboratory, AFSC
ATTN: SUL

Commander
ASD
ATTN: Technical Library

HQ USAF/IN
ATTN: INATA

Commander
Rome Air Development Center, AFSC
ATTN: EMTLD, Doc. Library

Commander in Chief
Strategic Air Command
ATTN: NRI-STINFO, Library

DEPARTMENT OF ENERGY

Department of Energy
Albuquerque Operations Office
ATTN: Doc. Con. for Tech. Library

Department of Energy
Division of Headquarters Services
Library Branch G-043
ATTN: Doc. Con. for Class. Tech. Lib.

Department of Energy
Nevada Operations Office
ATTN: Doc. Con. for Tech. Library

University of California
Lawrence Livermore Laboratory
ATTN: Doc. Con. for Tech. Info. Dept.

DEPARTMENT OF ENERGY (Continued)

Los Alamos Scientific Laboratory
ATTN: Doc. Con. for Reports Lib.

Sandia Laboratories
Livermore Laboratory
ATTN: Doc. Con. for Tech. Lib.

Sandia Laboratories
ATTN: Doc. Con. for 3141, Sandia Rpt. Coll.

OTHER GOVERNMENT AGENCY

Department of the Interior
Bureau of Mines
ATTN: Tech. Lib.

DEPARTMENT OF DEFENSE CONTRACTORS

Aerospace Corp.
ATTN: Tech. Info. Services

Agbabian Associates
ATTN: M. Agbabian

Avco Research & Systems Group
ATTN: A830, Research Lib.

Battelle Memorial Institute
ATTN: Tech. Lib.

BDM Corp.
ATTN: Tech. Lib.

Boeing Co.
ATTN: Aerospace Library

Calspan Corp.
ATTN: Tech. Lib.

Cambridge Acoustical Assoc., Inc.
ATTN: M. Junger

Civil/Nuclear Systems Corp.
ATTN: T. Duffy

Columbia University
Dept. of Civil Engineering
ATTN: F. Dimaggio
ATTN: H. Bleich

University of Denver
Colorado Seminary
Denver Research Institute
ATTN: Sec. Officer for F. Venditti

EG&G Washington Analytical Services Center, Inc.
ATTN: Tech. Lib.

General Dynamics Corp.
Electric Boat Division
ATTN: L. Chan

General Electric Co.
TEMPO Center for Advanced Studies
ATTN: DASIAC

IIT Research Institute
ATTN: Tech. Lib.

DEPARTMENT OF DEFENSE CONTRACTORS (Continued)

Institute for Defense Analyses
ATTN: IDA Librarian, R. Smith

Kaman AviDyne
Division of Kaman Sciences Corp.
ATTN: Tech. Lib.
ATTN: F. Criscione
ATTN: G. Zartarian

Kaman Sciences Corp.
ATTN: Library

Lockheed Missiles & Space Co., Inc.
ATTN: Tech. Lib.

Lockheed Missiles & Space Co., Inc.
ATTN: Tech. Info. Ctr.
ATTN: T. Geers
ATTN: K. Park
ATTN: C. Felippa
ATTN: J. DeRuntz

University of Maryland
Dept. of Civil Engineering
ATTN: B. Berger

Merritt CASES, Inc.
ATTN: Tech. Lib.

Nathan M. Newmark
Consulting Engineering Services
ATTN: N. Newmark

Physics International Co.
ATTN: Doc. Con. for Tech. Lib.

Polytechnic Institute of New York
ATTN: J. Klosner

Pacifica Technology
ATTN: J. Kent

R&D Associates
ATTN: Tech. Lib.

Science Applications, Inc.
ATTN: Tech. Lib.

SRI International
ATTN: B. Gasten
ATTN: G. Abrahamson

Systems, Science & Software, Inc.
ATTN: Tech. Lib.

Terra Tek, Inc.
ATTN: Tech. Lib.

Tetra Tech, Inc.
ATTN: Tech. Lib.
ATTN: Li-San Hwang

TRW Defense & Space Sys. Group
ATTN: Tech. Info. Center

Weidlinger Assoc., Consulting Engineers
ATTN: M. Baron

Weidlinger Assoc., Consulting Engineers
ATTN: J. Isenberg